Integrin regulation by tissue factor promotes cancer stemness and metastatic dissemination in breast cancer

Unlu, B.; Kocaturk, B.; Rondon, A.M.R.; Lewis, C.S.; Swier, N.; Akker, R.F.P. van den; ... ; Versteeg, H.H.

ARTICLE

Integrin regulation by tissue factor promotes cancer stemness and metastatic dissemination in breast cancer

Betül Ünlü[1], Begüm Kocatürk[1], Araci M. R. Rondon[1], Clayton S. Lewis[2], Nathalie Swier[1], Rob F. P. van den Akker[1], Danielle Krijgsman[3], Iris Noordhoek[3], Erik J. Blok[3], Vladimir Y. Bogdanov[2], Wolfram Ruf[4,5], Peter J. K. Kuppen[3] and Henri H. Versteeg[1]✉

Tissue Factor (TF) is the initiator of blood coagulation but also functions as a signal transduction receptor. TF expression in breast cancer is associated with higher tumor grade, metastasis and poor survival. The role of TF signaling on the early phases of metastasis has never been addressed. Here, we show an association between TF expression and metastasis as well as cancer stemness in 574 breast cancer patients. In preclinical models, blockade of TF signaling inhibited metastasis tenfold independent of primary tumor growth. TF blockade caused a reduction in epithelial-to-mesenchymal-transition, cancer stemness and expression of the pro-metastatic markers Slug and SOX9 in several breast cancer cell lines and in ex vivo cultured tumor cells. Mechanistically, TF forms a complex with β1-integrin leading to inactivation of β1-integrin. Inhibition of TF signaling induces a shift in TF-binding from α3β1-integrin to α6β4 and dictates FAK recruitment, leading to reduced epithelial-to-mesenchymal-transition and tumor cell differentiation. In conclusion, TF signaling inhibition leads to reduced pro-metastatic transcriptional programs, and a subsequent integrin β1 and β4-dependent reduction in metastasic dissemination.

Oncogene (2022) 41:5176–5185; https://doi.org/10.1038/s41388-022-02511-7

INTRODUCTION

Despite early diagnosis and improved treatment, breast cancer is still one of the leading causes of cancer-related deaths in women with nearly 40% of all breast cancer patients have regional (30.8%) or distant (6.2%) metastases [1]. Metastasis is promoted by epithelial-to-mesenchymal-transition (EMT), in which cell-cell contact is lost and a spindle-shape morphology is acquired with enhanced migratory and invasive properties. This EMT program is under control of EMT-related transcription factors, like members of the SNAIL, TWIST and ZEB families [2, 3]. It becomes more evident that there is an intimate relationship between EMT and cancer stem cells (CSCs) required for successful metastasis [4–6]. CSCs comprise a sub-population of the tumor with the ability to self-renew and seed new tumors with an enhanced resistance towards chemotherapy [7]. CSCs in breast cancer may be identified based on the expression of surface markers $CD133^+$, $CD44^+/CD24^-$ and/or the intracellular protein aldehyde dehydrogenase 1 (ALDH1) [8]. The current hypotheses are either that (i) cells that have undergone EMT de-differentiate into CSCs or (ii) CSCs start expressing EMT-associated markers, after which they metastasize [9]. One protein that is suggested to drive cancer stemness is the coagulant protein Tissue Factor (TF) [10].

Hemostasis is critically involved in tumor progression. For instance, primary hemostasis, i.e. platelet aggregation, primes tumor cells for metastasis by inducing TGFβ/NF-kB pathways [11]. Nevertheless, secondary hemostasis, i.e., blood coagulation, often plays roles in tumor progression as well. TF is the initiator of the coagulation pathway and is expressed on sub-endothelial cells. It activates its ligand factor VII (FVII) after vessel injury, coagulation factor X (FX) is then activated leading to prothrombin cleavage, activation of platelets and fibrin deposition in order to close the wound. However, TF is also synthesized by breast tumor cells, and this expression has been found to associate with higher tumor grade, increased angiogenesis, reduced survival, increased invasive and metastatic behavior [12].

Classically, it has been thought that TF influences tumor progression via two distinct processes. First, TF in complex with FVIIa induces (i) direct cellular signaling via protease activated receptor-2 (PAR2) and (ii) indirect TF signaling through crosstalk with integrins, to promote tumor angiogenesis, growth and migration, respectively [13, 14]. TF signaling also promotes invasion through increased production of matrix metalloproteinases (MMPs) allowing tumor cells to escape the tumor environment. Upon entering the bloodstream, coagulant functions of TF become key, as it forms a fibrin/platelet-rich shield around circulating tumor cells. This prevents attack from the immune system, and thereby promotes survival of metastatic cells [14, 15]. While TF coagulant function clearly adds to metastatic potential, the significance of TF signaling in the early events leading to metastasis has not been addressed in vivo.

[1]Einthoven Laboratory for Experimental Vascular Medicine, Department of Internal Medicine, Leiden University Medical Center, Leiden, The Netherlands. [2]Division of Hematology/Oncology, Department of Internal Medicine, College of Medicine University of Cincinnati, Cincinnati, OH, USA. [3]Department of Surgery, Leiden University Medical Center, Leiden, The Netherlands. [4]Department of Immunology and Microbiology, The Scripps Research Institute, La Jolla, CA, USA. [5]Center for Thrombosis and Hemostasis, Johannes Gutenberg University Medical Center, Mainz, Germany. ✉email: h.h.versteeg@lumc.nl

Received: 13 June 2019 Revised: 6 October 2022 Accepted: 11 October 2022
Published online: 21 October 2022

In this study, we have investigated whether TF signaling impacts metastasis and the cellular processes underlying metastasis, in vitro and in vivo, with a special focus on integrin regulation by TF.

RESULTS

TF expression associates with metastasis in estrogen receptor negative tumors

We first investigated clinical associations between TF expression, stratified for low or high TF (Fig. S1), and metastasis-free survival of breast cancer patients. Tumor specimens from 574 breast cancer patients were stained for TF and stratified for Estrogen Receptor (ER) expression. Expression of TF in ER+ tumors did not associate with metastasis-free survival (Fig. 1A). However, a significant association between high TF levels and metastasis in ER- tumors was observed in the first 5 years after diagnosis (Fig. 1B). Importantly, similar observations were made in tumors from patients that had not yet received therapy (Fig. S2), ruling out an effect of therapy on these associations. Cancer stem cells (CSCs) play a fundamental role in metastasis, thus we also determined associations between TF expression and the CSC marker ALDH1. We observed a significant association (Fig. 1C) that was even stronger in ER- and PgR- cells (Fig. S3).

Inhibition of TF signaling reduces metastasis in vivo

Our own work in patient material and in in vitro models [10] indicate a role for TF signaling in CSCs and suggest that metastasis may be critically dependent on TF signaling. To further investigate the role of TF signaling in metastasis, the highly aggressive and triple-negative MDA-MB-231-mfp cell line that expresses TF [16] was grafted orthotopically in the mammary gland. In the presence of Mab-10H10—a specific inhibitor of TF signaling—a fivefold decrease of tumor growth was observed in comparison to IgG control (Fig. 1D) that was not due to potential cytotoxic effects (results not shown). After mice were sacrificed, lungs were processed to study the presence of human cells using qPCR. Strikingly, the presence of Mab-10H10 reduced metastatic dissemination 100-fold (Fig. 1E). Immunohistochemistry on isolated lungs substantiated this (Fig. S4A). Fibrin formation and platelet aggregation on the surface of metastatic tumor cells play a

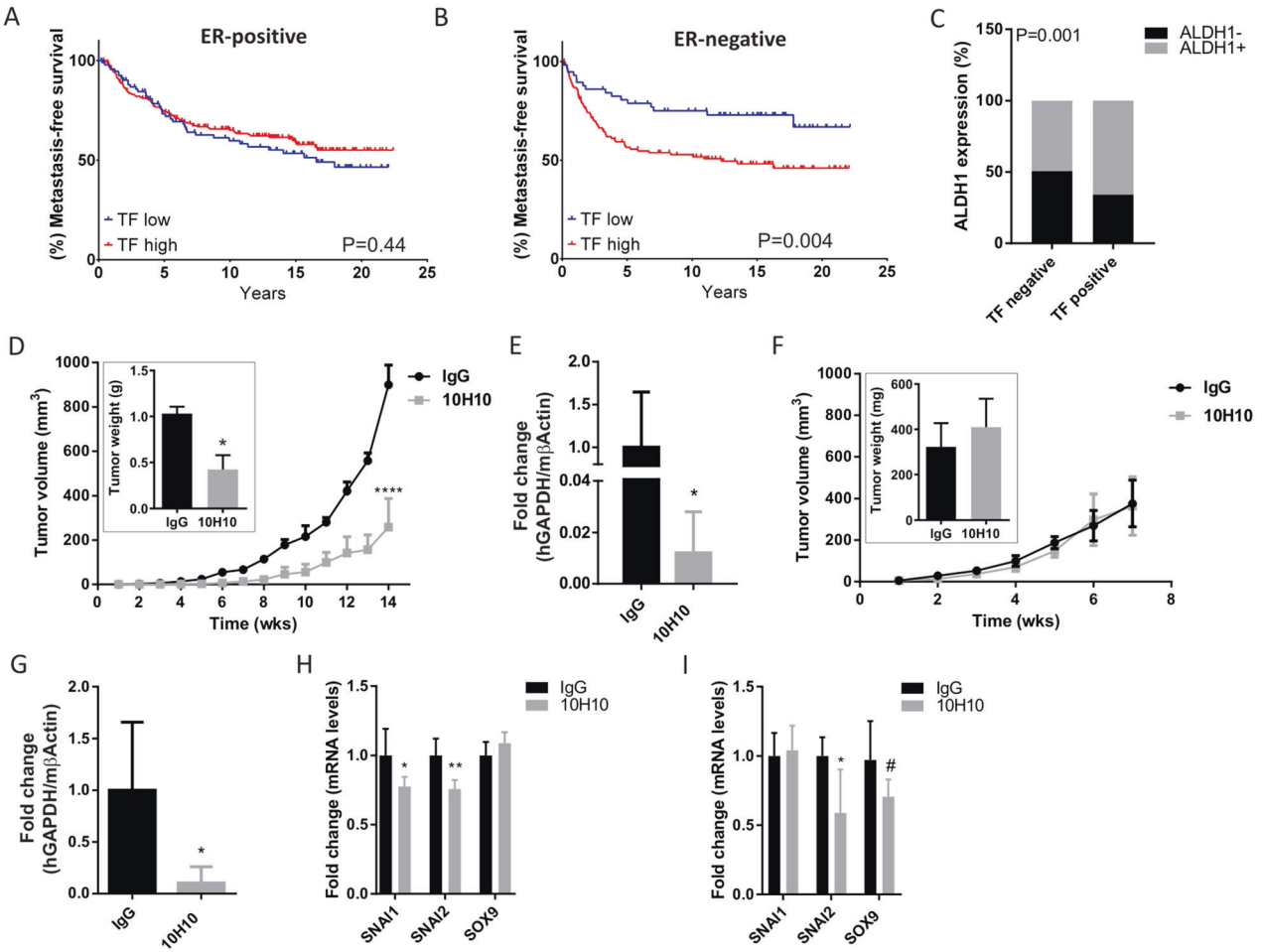

Fig. 1 TF associates with metastasis in patients with ER-negative breast tumors, and TF signaling induces metastasis. A Kaplan–Meier analysis of metastasis-free survival in breast cancer patients with ER-positive tumors, stratified for TF expression. **B** Kaplan–Meier analysis of metastasis-free survival in breast cancer patients with ER-negative tumors, stratified for TF expression. **C** Association between expression of the breast cancer stem cell marker ALDH1 and TF. TMA consisted of $N = 574$ breast tumor specimens, $N = 146$ TF negative, and $N = 308$ TF positive tumors, assessment of associations were performed using SPSS. **D** MDA-MB-231-mfp cells were orthotopically injected in the presence of 500 μg IgG control or Mab-10H10 antibody in NOD-SCID mice ($n = 4$). Tumor growth was monitored until week 14. Mean and SD are shown. **E** Lungs from NOD-SCID mice were analyzed by qPCR to assess metastasis by determining human GAPDH levels corrected for mouse β-actin levels. **F** MDA-MB-231-mfp cells were orthotopically injected in the presence of 500 μg IgG control or Mab-10H10 antibody in NOD-SCIDγ mice ($n = 5$). **G** Lungs from NOD-SCIDγ mice were analyzed by qPCR to assess metastasis by determining human GAPDH levels corrected for mouse β-actin levels. All tumors were analyzed by qPCR for the mRNA expression of *SNAI1*, *SNAI2*, and *SOX9* from NOD-SCID (**H**) and NOD-SCIDγ mice (**I**). $^{\#}P < 0.10$; $^{*}P < 0.05$; $^{**}P < 0.01$; $^{***}P < 0.001$; $^{****}P < 0.0001$.

key role in TF-mediated metastasis, as these TF-dependent processes can efficiently block tumor cell eradication by natural killer (NK) cells [17]. To further evaluate the contribution of TF signaling to metastasis, independent of fibrin formation and platelet aggregation, we repeated the in vivo experiment in NK cell deficient mice. Tumor volumes were equal after 7 weeks of inoculation (Fig. 1F). However, there was a significant 10-fold reduction of metastatic dissemination to the lungs when tumor cells were grafted orthotopically in the presence of Mab-10H10 (Figs. 1G, S4B). These data suggest that TF signaling, independent of NK function, is directly responsible for pro-metastatic events in the primary tumor. qPCR analysis of the tumors for EMT-associated markers showed a significant reduction in SNAIL (*SNAI1*) and SLUG (*SNAI2*) mRNA levels, in a NOD-SCID setting (Fig. 1H). While a significant downregulation of *SNAI2* was observed in tumors grown in NK cell deficient mice, *SNAI1* expression remained unaffected and a trend towards decreased *SOX9* expression was present (Fig. 1I).

Blockade of TF signaling reduces CSC programs in vitro

To investigate if blockade of TF signaling results in a decreased EMT transcription program in vitro, MDA-MB-231-mfp cells were pre-treated with antibodies to inhibit TF signaling. As expected, well-established downstream targets of TF signaling, *CXCL8*, *CXCL1*, and *VEGF*, were significantly decreased (Fig. 2A). Although treatment of MDA-MB-231-mfp cells with Mab-10H10 had no effect on *SNAI1* expression, *SNAI2*, *SOX9* and *MMP9* were significantly downregulated by 2-fold at mRNA levels (Fig. 2B, C). Furthermore, similar results were obtained at protein level, with lowered abundance of Snail and SOX9 protein levels (Fig. 2D). Importantly, 10H10 induced similar decreases in BT-20, MDA-MB-

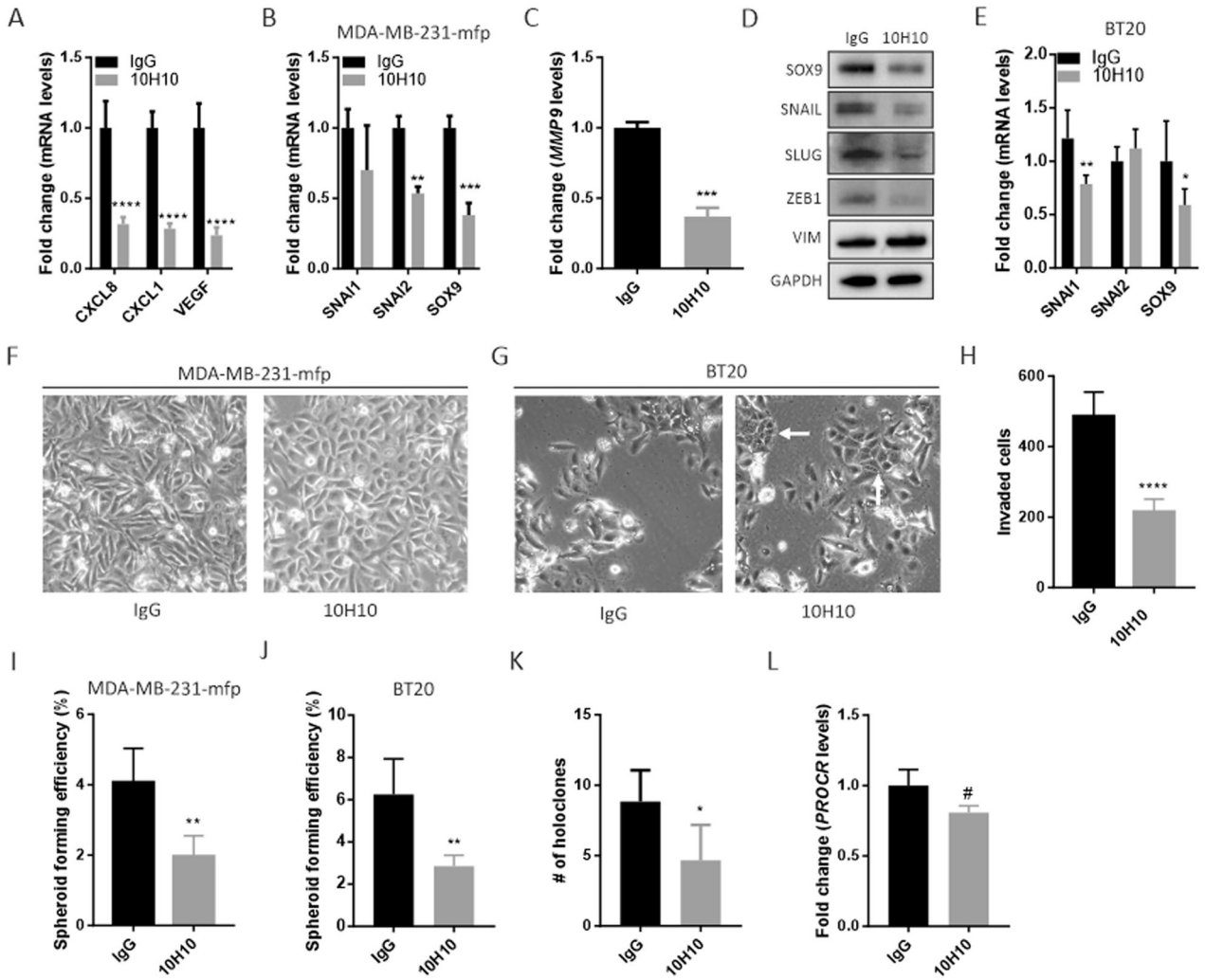

Fig. 2 TF signaling inhibition reduces EMT and CSC program in vitro. A Treatment of MDA-MB-231-mfp cells with 50 µg/ml Mab-10H10 for 72 h reduces mRNA expression of *CXCL8*, *CXCL1* and *VEGF*. **B** Decreased mRNA expression of EMT-associated markers *SNAI2* and *SOX9* after 72 h treatment with Mab-10H10 in MDA-MB-231-mfp cells. **C** Mab-10H10 treatment of MDA-MB-231-mfp downregulates *MMP9* expression. **D** Expression of SOX9 and Snail antigen levels after 72 h antibody treatment. **E** Decreased mRNA expression of EMT-associated markers *SNAI1* and *SOX9* after 72 h treatment with Mab-10H10 in BT-20 cells. Morphological changes were observed during cell culture when MDA-MB-231-mfp cells (**F**) or BT-20 cells (**G**) were treated with 50 µg/ml Mab-10H10. **H** Invasion assay of MDA-MB-231-mfp cells in the presence of 50 µg/ml IgG control or Mab-10H10 antibody ($n = 5$ per condition). **I** 500 MDA-MB-31-mfp cells were plated into ultra low-attachment 96-well plates in the presence of 50 µg/ml IgG control or Mab-10H10 antibody and cultured in tumor sphere medium for 14 days ($n = 6$). Tumor spheres with a surface larger than 2000 µm^2 were counted. **J** Tumor sphere experiments as in I, but using BT-20 cells. **K** Suppressive effect of TF signaling inhibition on colony formation capacity of MDA-MB-231-mfp cells. Colonies consisting over 50 cells with a holo-type phenotype were counted ($n = 6$). **L** *PROCR* expression after 72 h Mab-10H10 treatment. Data shown are the mean ± SD, three independent experiments were performed in technical triplicates, and statistical significance was analyzed using Student's *t* test for two or two-way ANOVA for three data sets. $^{\#}P < 0.10$; $^{*}P < 0.05$; $^{**}P < 0.01$; $^{***}P < 0.001$; $^{****}P < 0.0001$.

436 and Hs578T breast cancer cell lines (Figs. 2E, S5A–I). Moreover, while mRNA of the EMT transcription factor Twist was undetectable in MDA-MB-231-mfp and BT-20 cells, Mab-10H10 reduced *TWIST* mRNA levels in MDA-MB-436 cells (Fig. S5E). Additionally, TF expression in our cohort of 574 breast cancer patients associated with high combined expression of *SNAI1* and *TWIST*, and with *SOX9*, but only in tumors that were ER- (Tables S2, S3). The observed EMT program coincided with appearance of a epithelial-like population, compared to cultures treated with control IgG (Fig. 2F, G). MMP9 is a protein involved in the degradation of the extracellular matrix (ECM), allowing tumor cells to escape the primary tumor. In line with reduced *MMP9* expression levels upon Mab-10H10 treatment, a 2-fold reduction in invasive capacity of MDA-MB-231mfp was observed using invasion assays compared to control IgG (Fig. 2H). Since SOX9 is considered a driver of CSC-genesis [18] and a significant decrease in expression of *SOX9* was observed in Mab-10H10-treated MDA-MB-231-mfp cells, we hypothesized diminished CSC properties of these cells. Cells were seeded on low-attachment plates in order to evaluate mammosphere formation (Fig. S6A). As expected, less tumor colonies were counted after Mab-10H10 treatment by at least twofold in several breast cancer cell lines, (Figs. 2I, J, S5J, K). Additionally, Mab-10H10-treated cells showed a reduction in holoclone formation (Figs. 2K, S6B), the most aggressive clone-type, with highly proliferative properties and self-renewal capacity [19]. Furthermore, an in-trend decrease in the expression of Endothelial Protein C Receptor, (EPCR; encoded by *PROCR*), a CSC marker in triple-negative breast cancer [20] when TF signaling was inhibited (Fig. 2L). In conclusion, TF signaling inhibition in vitro decreases both EMT-associated expression profiles and CSC behavior.

Mab-10H10-treated tumors are less tumorigenic ex vivo

To investigate if blockade of TF signaling resulted in a permanent change of malignant tumor cell phenotype, MDA-MB-231-mfp-derived tumors were collected and cultured ex vivo. Similar to cells treated in vitro, tumor cells isolated from Mab-10H10-treated mice showed a morphological change towards an epithelial-like phenotype (Fig. 3A), that was persistent and still observed after 10 weeks of culturing (Fig. S7). Ingenuity pathway profiling after gene array analysis indicated alterations in expression profiles that associate with morphology, cellular development, function and cell-to-cell interactions (Table S4). This epithelial-like phenotype was supported by an increased expression of the adherens junction- and desmosome-associated genes *JUP* (γ-catenin), *PLEKHA7* (pleckstrin) and *DSP* (desmoplakin)—all contributing to epithelial homeostasis (Fig. 3B). While in vitro treatment of MDA-MB-231-mfp with Mab-10H10 did not lead to apparent changes in expression of these genes, Mab-10H10 increased *JUP* expression in MDA-MB-436 in vitro (Fig. S8). Expression of the EMT marker *SNAI1*, was decreased in Mab-10H10 ex vivo cells, with a trend towards less expression of *SOX9* and *VIM* (Fig. 3C). Snail levels were significantly decreased by 2-fold in Mab-10H10 ex vivo cells, while β1-integrin and TF expression remained unchanged (Fig. 3D). Mab-10H10 ex vivo cells showed diminished *MMP9* mRNA expression (Fig. 3E). As expected, a significant 8-fold reduction of cell invasion was observed compared to control IgG ex vivo cells (Fig. 3F, G). Mab-10H10 ex vivo cells showed reduced CSC activity, because less spheroids and holoclones were counted (Fig. 3H, I). Additionally, *PROCR* expression was reduced in Mab-10H10 cells (Fig. 3J). Thus, ex vivo cells of tumors treated with Mab-10H10 display changes in cell phenotype, with decreased EMT and CSC features, which persist during culture in vitro.

TF regulates the location of integrins at the plasma membrane

Thus far, we have shown that TF signaling is involved in EMT/CSC programs and in pro-metastatic events. TF influences migration and cell adhesion via the regulation of integrins, that is independent of PAR2-mediated signaling [21]. Therefore, to

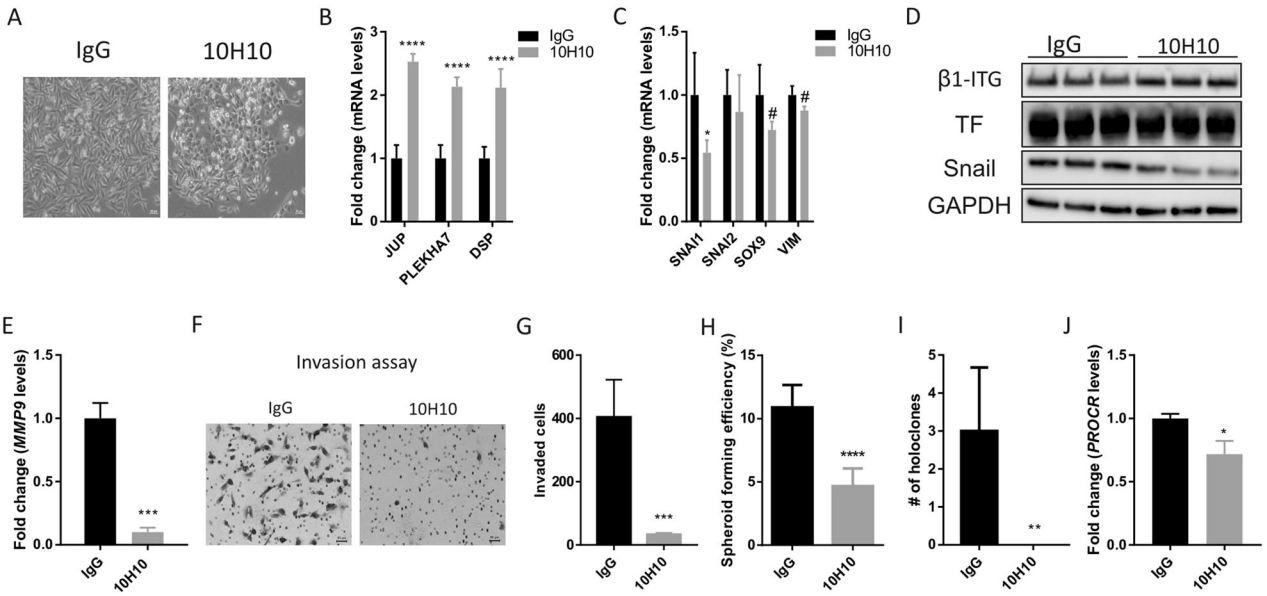

Fig. 3 Blockade of TF signaling reduces EMT and CSC program in ex vivo cells. A Morphological changes were observed during cell culture of MDA-MB-231-mfp ex vivo cells that were isolated from tumors. Scale bar = 50 µm. **B**, **C** Transcription levels of adherens junction associated markers *JUP*, *PLEKHA7, DSP* (**B**), and EMT-associated markers *SNAI1*, *SNAI2*, *SOX9* and *VIM* (**C**) in IgG or Mab-10H10 ex vivo cells measured using qPCR. **D** Protein levels in ex vivo cells derived from control or Mab-10H10 tumors. **E** mRNA level of *MMP9* in IgG and 10H10 ex vivo cells. **F** Matrigel invasion assay with ex vivo IgG and Mab-10H10 cells ($n = 5$). Crystal violet staining of invaded cells are shown. **G** Data are represented as mean ± SD of cell numbers that invaded in total per well ($n = 4$). **H** 500 ex vivo cells were plated into ultra low-attachment 96-well plates and cultured in tumor sphere medium for 14 days ($n = 6$). Tumor sphere numbers were counted with a surface larger than 2000 µm^2. **I** Colonies (>50 cells) with a holoclone phenotype were counted ($n = 6$). **J** mRNA transcription levels of *PROCR* in IgG or Mab-10H10 ex vivo cells. Data shown are the mean ± SD, three independent experiments were performed in technical triplicates, and statistical significance was analyzed using Student's *t* test for two or two-way ANOVA for three data sets. $^{\#}P < 0.15$; $^{*}P < 0.05$; $^{**}P < 0.01$; $^{***}P < 0.001$; $^{****}P < 0.0001$.

mechanistically unravel how TF signaling affects CSCs we focused on interactions with integrins. As integrins enable the cells to bind ECM, mediate migration and regulate CSCs [22], we addressed whether inhibition of TF signaling influences integrin behavior. First, we investigated the effects of integrin activation on EMT programs using different ECM components, i.e., vitronectin that binds αvβ3-integrin [23] and laminin, binding many β1-integrin dimers and α6β4-integrin [24]. Cells were seeded on vitronectin- or laminin-coated plates and treated with Mab-10H10 or IgG control, followed by mRNA analysis of EMT-associated factors. Inhibition of TF signaling resulted in a 2-fold reduction of *SNAI1/2* expression on vitronectin coated plates, while expression was unchanged when cells were seeded on laminin (Fig. S9A, B). Effects of different ECM components on *SOX9* mRNA expression were even more pronounced, with a 90% reduction on vitronectin, (Fig. S9C) with similar trends in *VIM* and *MMP9* expression after treatment with Mab-10H10 on vitronectin but not on laminin (Fig. S9D, E). Finally, Mab-10H10 treatment also had more pronounced effects on *SNAI1*, *SOX9* and *VIM* in BT-20 cells cultured on vitronectin, but not on laminin (Fig. S10).

Next, we investigated how integrins influence TF signaling mediated EMT- and CSC-associated behavior. Cells were treated with Mab-10H10 or IgG, and then lysed in Brij35-buffer that dissolves non-raft, cholesterol-poor cell membrane fractions [25]. β1-integrins were immunoprecipitated with various β1-integrin conformation-recognizing antibodies, after which precipitates were analyzed for β1-integrin and TF. Inhibition of TF signaling in MDA-MB-231-mfp and BT-20 cells resulted in an ~2-fold reduction of TF/β1-integrin complexes in the Brij35-soluble fraction (Figs. 4A, S11), while β1-integrin expression remained equal. Interestingly, pull down assays with AIIB2 (total β1-integrin) and HUTS21 (active β1-integrin) co-immunoprecipitated FAK and Src when MDA-MB-231-mfp cells were treated with Mab-10H10, suggesting an active β1-integrin conformation. The β1-integrin antibody TS2/16, that activates β1 on intact cells and immunoprecipitates the TF-FVIIa complex [26], did not immunoprecipitate FAK/Src in the presence of Mab-10H10, indicating that FVIIa is not involved in the effect of Mab-10H10. In addition, immunofluorescent staining for FAK in MDA-MB-231-mfp cells treated with Mab-10H10 demonstrated the formation of focal adhesions at the plasma membrane (Fig. 4B), confirming FAK activation in the presence of Mab-10H10. Inhibition of FAK resulted in a significant increase of *SNAI1/2* expression, while *SOX9* remained unaffected (Fig. 4C). Mab-10H10 treatment decreased α2- and α3-integrin heterodimers with β1-integrin and precipitation of TF in the Brij35-soluble fraction (Fig. 4D). In contrast, precipitation of TF was increased markedly by Mab-10H10 treatment in the α6-integrin pull down from cholesterol-rich membrane fraction—Brij-58 soluble—and less so in the non-raft fractions. Total expression of α-integrin subunits did not change upon Mab-10H10 treatment (Fig. 4E). These data suggest that blockade of TF signaling causes a shift of TF towards α6β4-integrin into the cholesterol-rich membrane fractions. These data also indicate that integrin activation is induced by Mab-10H10 treatment to suppress the CSC phenotypes. Consistently, inhibition of β1-integrin—but not PAR2—increased mammosphere formation in cells treated with Mab-10H10 (Fig. 4F). Treatment of MDA-MB-231-mfp cells with the PAR2 antagonist GB83 showed similar results as those observed after antibody-mediated inhibition (Fig. 4G). Additionally, mRNA expression profiles of EMT-related genes were examined after inhibition of β1-integrin and PAR2. Inhibition of either receptor resulted in increased *SNAI2* expression. A trend towards increased *SOX9* expression was observed when β1-integrin was inhibited with Mab-AIIB2, while inhibition of PAR2 had no effect on *SOX9* transcription levels (Fig. 4H). Finally, inhibition of β1-integrin using shRNA approaches led to enhanced *SNAI2* but not *SOX9* levels (Fig. 4I). These data suggest that TF signaling mediates the localization and function of β1-integrin within the cell membrane. Furthermore, disruption of the TF/β1-integrin complex results in an epithelial-like morphology with less tumorigenic properties.

TF signaling keeps cells in a mesenchymal state via suppression of β4 integrin expression

How integrins contribute to cancer stem cell behavior is poorly understood. Recently, Bierie and co-workers showed that α6β4-integrin distinguishes subpopulations in mesenchymal triple-negative breast cancer [27]. MDA-MB-231 cells that are β4-integrin-positive associated with a more epithelial morphology and decreased tumorigenic properties. We found that treatment with Mab-10H10 influenced β4-integrin expression in our highly aggressive MDA-MB-231-mfp cell line. After Mab-10H10 treatment, magnetic activated cell sorting (MACS) isolated the same number of β1-integrin positive cells and CSC marker CD133, but TF signaling inhibition increased the number of β4-integrin-positive cells 15-fold (Fig. 5A–C). After MACS sorting these cells were cultured for 1 week. Whereas the cells displaying low β4-integrin expression from control IgG treated cells had mesenchymal-like morphology, an epithelial-like morphology was observed in the β4-integrin^{high} population isolated from Mab-10H10-treated cells (Fig. 5C). Immunoprecipitation of β4-integrin confirmed the increased association of α6-integrin and TF in Mab-10H10-treated cells. Furthermore, increased FAK and Src antigen were co-precipitated with integrin β4-after Mab-10H10 treatment (Fig. 5D). Diminished TF signaling caused a morphological change into less tumorigenic cells via increased α6β4-integrin expression and activation at the cell surface. Interestingly, β4-integrin expression was higher in Mab-10H10 ex vivo cells (Fig. 5E, F), whereas TF and β1-integrin expression remained unchanged (Fig. 5D). In vitro incubation of MDA-MB-436 cells with Mab-10H10 similarly induced β4-integrin transcript, (Fig. S12). Finally, shRNA-mediated knockdown of β4-integrin enhanced mRNA levels of *SOX9* but not *SNAI2*.

DISCUSSION

TF expression is linked to decreased metastasis-free survival in lung, gastric, pancreatic and colorectal cancer [28–31], but associations between TF and metastasis in breast cancer patients have remained obscure [32–34]. In this study an association could be found when breast tumors were stratified for ER status, with a significant association in ER- tumors (Fig. 1A, B). An association was not found in ER + tumors, possibly reflecting the different biological and clinical characteristics of these tumor types. In support, a recent study demonstrates increased TF expression in triple-negative breast cancer [35], a highly invasive subtype of breast cancer that is associated with poor survival [36]. Of note, in our work we used several breast cancer cells constituting triple-negative breast cancer cell lines and in these cells, TF supports invasion and metastatic dissemination in an ER- setting.

When MDA-MB-231-mfp cells were orthotopically grafted in the presence of the TF signaling inhibitor Mab-10H10 a dramatic decrease in metastatic dissemination was observed. As this antibody does not inhibit coagulant properties of TF, our results demonstrate that in an orthotopic setting, TF signaling impacts metastasis. It should also be noted that TF signaling promoted metastatic dissemination both in NK cell deficient and proficient mice (Fig. 1D–G). This is of importance as previous work making use of experimental metastasis models -relying on injection of cancer cells into the bloodstream- suggested that in this setting evasion of NK cells was dependent on coagulant function of TF. Nevertheless, experimental metastasis does not fully recapitulate metastasis as primary tumor growth, degradation of the basement membrane, local invasion and intravasation are circumvented [37]. Primary tumor growth was unaffected by Mab-10H10 treatment in the absence of NK cells, raising the possibility that Mab-10H10 treatment in NK proficient mouse models elicits antibody-dependent cellular cytotoxicity (ADCC) [14, 38]. We further note that the current data do not unequivocally show which aspects of metastatic dissemination in vivo are affected by Mab-10H10, but

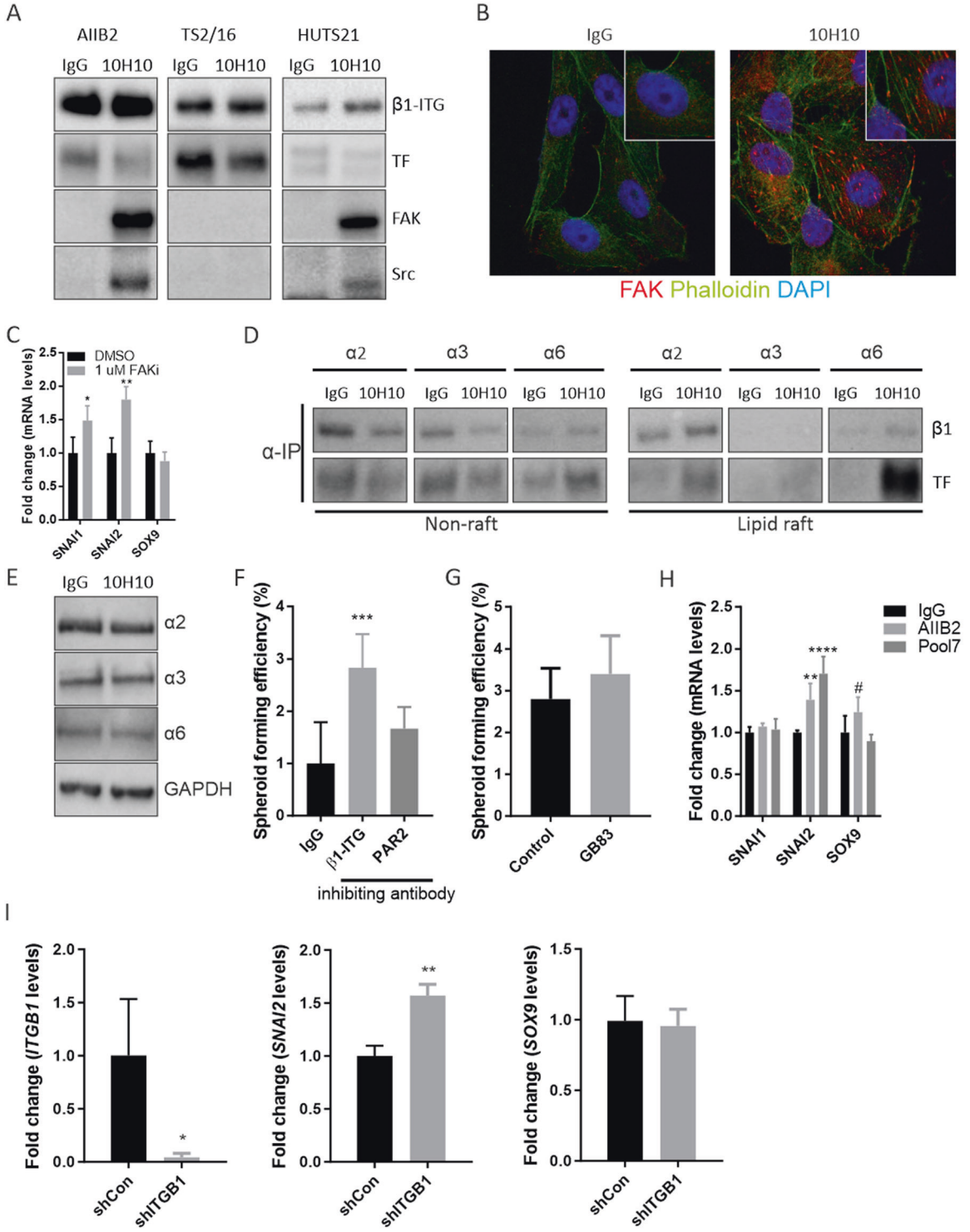

in vitro, Mab-10H10 inhibited invasion (Fig. 2H), which is key in metastatic dissemination.

In addition, our experiments demonstrated that TF signaling affects early metastatic events such as EMT. Mab-10H10 treatment resulted in a downregulation of EMT transcription factors Snail and/or Slug (Fig. 2B, E). As TF appears to influence EMT, which is dynamically linked to CSCs [10], and expression of the CSC effector SOX9 was significantly reduced in our in vitro model after Mab-10H10 treatment, the question arises as to whether TF expression is associated with CSCs. Indeed, our clinical data demonstrates an association between TF levels and ALDH1, a marker for CSCs (Fig. 1C). In support, Mab-10H10 treatment resulted in decreased mammosphere and holoclone formation (Fig. 2I–K), suggesting that TF signaling specifically influences cancer stem cells. Shaker et al. have previously demonstrated that TF expression promotes CSCs in breast cancer, nevertheless, our study is the first to show that the involvement of TF in CSC maintenance is dependent on its signaling properties [10]. Collectively, these data show that TF signaling is directly responsible for NK-independent metastasis via modulation of the EMT and CSC program.

Fig. 4 TF determines β1-integrin localization in the cell membrane. A Pull down assay of β1-integrins with AIIB2, TS2/16 and HUTS21 after 72 h treatment with IgG or Mab-10H10. Co-immunoprecipitation was analyzed with Western Blot for β1-integrin, TF, FAK and Src. **B** Blockade of TF signaling increases focal adhesion complex formation after 72 h Mab-10H10 treatment. MDA-MB-231-mfp cells were stained for FAK. **C** mRNA expression of *SNAI1, SNAI2* and *SOX9* in MDA-MB-231-mfp cells after 72 h treatment with control (DMSO) or 1 μM FAK II inhibitor. **D** Localization of α2-, α3- and α6-integrin was studied in non-raft and lipid raft fractions after 72 h Mab-10H10 treatment. Precipitates were analyzed for the presence of β1-integrin and TF on western blot. **E** Western blotting for α-integrin subunits on total cell lysates showed no changes in antigen levels after blockade of TF signaling. **F** 500 MDA-MB-231-mfp cells were plated into ultra low-attachment plates in the presence of 50 μg/ml control IgG, Mab-AIIB2 (β1-integrin) or Pab-pool7 (PAR2) antibody and cultured in tumor sphere medium for 14 days. Tumor spheres with a surface larger than 2000 μm^2 were counted. **G** 500 cells were plated into ultra low-attachment plates in the presence of control (DMSO) or 10 μM PAR2 antagonist (GB83) and cultured in tumor sphere medium for 14 days. Tumor sphere numbers were counted with a surface larger than 2000 μm^2. **H** Transcription levels of *SNAI1, SNAI2* and *SOX9* in the presence of control IgG, Mab-AIIB2 (β1-integrin) or Pab-pool7 (PAR2) antibody for 72 h. **I** Knockdown of β1-integrin and effects on *SNAI2* and *SOX9* mRNA levels. Pull down assays were repeated at least three times. Data shown are the mean ± SD, three independent experiments in triplicate, and statistical significance was analyzed using Student's *t* test for two data sets or two-way ANOVA for three or more data sets. *$P < 0.05$; **$P < 0.01$; ***$P < 0.001$; ****$P < 0.0001$.

An interesting observation in this study was a transient change in the morphology of in vitro 10H10-treated cells from a mesenchymal to an epithelial-like phenotype (Fig. 2F, G). Posttranslational decreases were observed in Snail and ZEB1 expression (Fig. 2D) and both transcription factors were previously shown to be essential for the establishment of an extremely tumorigenic hybrid epithelial/mesenchymal state. Thus, Mab-10H10 may specifically target cells in a hybrid E/M state.

When in vivo 10H10-treated cells were reisolated from tumors we observed partial morphological changes (i.e., a subset of cells showed an epithelial morphology) (Fig. 3A). However, in contrast to Mab-10H10 cells in vitro, ex vivo cells showed changes that were still present after 10 months of culture. We observed elevated β4-integrin expression, increased expression profiles of adherens junction and desmosome components and decreased expression of *SNAI1*, but not of *SNAI2* and *SOX9*. (Fig. 3B, C). Importantly, in an previous study, increases in *SNAI1* were associated with the presence of more tumorigenic epithelial/mesenchymal hybrid cells, suggesting that TF expression mediates this quasi-mesenchymal (hybrid E-M) state [27]. We further hypothesize that the tumor microenvironment may have driven the EMT state of our ex vivo cells to a permanent one, as a recent study shows that EMT stages are determined by the presence of stromal cells [39]. Indeed, in previous work by the group of Rak tumor cell TF expression and the microenvironment have been found to regulate each other [40].

Classically, TF mediates FVIIa-dependent activation of PAR2, however, inhibition of PAR2 did not impact spheroid forming efficiency (Fig. 4F, G). In addition, we performed our experiments in the absence of FVIIa making it unlikely that TF-dependent effects on EMT/CSC are FVIIa- or PAR2-mediated. Rather, we postulate that TF, in the context of EMT and CSC biology, regulates integrin function. EMT/CSC-associated markers were downregulated when TF/integrin crosstalk was inhibited with 10H10 on vitronectin (Fig. S9), an activator of β3- and β5-integrins [41]. Expression of these markers was already low when cells were seeded on laminin a ligand for β1-integrin [42], and expression was not further downregulated when TF signaling was inhibited. In addition, inhibition of β1-integrin resulted in increased *SNAI2* expression. These data suggest that β1-integrin is involved in TF signaling-dependent EMT and CSC transcriptional programs. Altogether, we hypothesize that TF/PAR-mediated signaling is required for angiogenesis and proliferation, while the TF/integrin axis is responsible for EMT and CSC.

To further delineate the nature of the β1-integrin/TF signaling pathway, β1-integrin immunoprecipitates were investigated. Mab-10H10 led to uncoupling of TF/β1-integrin complexes, as shown in this study (Fig. 4A) and previous studies [14]. This is in line with studies on the crystal structure of TF/ β1-integrin showing that Mab-10H10 blocks the putative β1-integrin binding site [43]. Furthermore, in the presence of Mab-10H10 increased binding of focal adhesion kinase to β1-integrin was observed, as well as increases in focal adhesion complexes and presence of actin fibers (Fig. 4A, B). This may be initiated by Mab-10H10 that shifts TF in a complex with α6β1-integrin—which may not be recognized by TS2/16—and recruits filamin and FAK through the cytoplasmic domain [44]. Further, this Mab-10H10 treatment resulted in an increase of the active β1-integrin conformation and a decrease in cancer stemness. Although α6β1-integrin has been implicated in CSC phenotypes [45], our data show that TF dictates FAK/Src recruitment to any α6-integrin heterodimer—including α6β4-integrin—that promotes differentiation. Thus, we postulate that Mab-10H10 reverses TF-dependent inhibition of β1-integrin, leading to focal adhesion assembly and an epithelial state.

The epithelial morphology may be further influenced by β4-integrin [46], as interaction of α6β4-integrin with CD151 increases cell adhesion and formation of hemidesmosomes, that mediates a stable cell attachment to the ECM [47]. Indeed, we observed a significant increase in cellular β4-integrin expression and physical interaction between TF and β4-integrin upon inhibition of TF signaling. We currently have no data to show how TF associates with β4-integrin in the presence of Mab-10H10, but it is reasonable to assume that it is distinct from the β1-integrin binding site. Also, β4-integrin expression, which was recently shown to be a negative marker for CSCs, discriminated between aggressive and less aggressive Mab-10H10-treated cells [27], and in our studies was negatively coupled to *SOX9* expression (Fig. 5C, G).

In conclusion, uncoupling of TF/β1-integrin signaling pathways, increases integrin β4 expression, decreases EMT/CSC programs, thereby suppressing metastases (Fig. 6). We posit that TF signaling may be an important target for the treatment of triple-negative breast cancer, and disruption of TF/β1-interactions may help to prevent relapse and increase overall survival.

MATERIALS AND METHODS

Reagents and cell culture

All breast cancer lines (all being triple negative, i.e., no expression of ER, PgR and Her2) were cultured in DMEM (41966-052, Life Technologies), supplemented with 10% FBS (10270-106, Gibco), 2 mM L-Glutamine (G7513-100ML, Sigma-Aldrich) and 1% penicillin/streptomycin (P4333-100ML, Sigma-Aldrich) at 5% CO_2, 37 °C. To coat culture plates with ECM components, vitronectin (V8379, Sigma-Aldrich) and supernatant from 804G cells for laminin condition were used. For antibody inhibition approaches anti-TF (Mab-10H10; mouse); anti-β1 integrin (Mab-AIIB2; rat); anti-PAR2 (Pab-pool7; mouse) and IgG control (TIB115) were prepared in-house [15]. For a list of all reagents used, please see Table S5.

Tissue microarray analysis

We made use of a previously described tissue array including material from 574 breast cancer patients [48]. Sections were immunohistochemically stained for TF (American Diagnostica, clone 4509), ALDH1 (Biosciences, BD 611195) and Sox9 (Merck-Millipore, AB5535) as described previously [49]. The percentage of TF, ALDH1 and SOX9 positive tumor cells was scored by two blinded observers. The percentage of TF and ALDH1 positive tumor cells were determined, and the negative tumors were deemed in the 1st quartile. Sox9 expression was determined as weak staining or strong staining. Slug, Snail

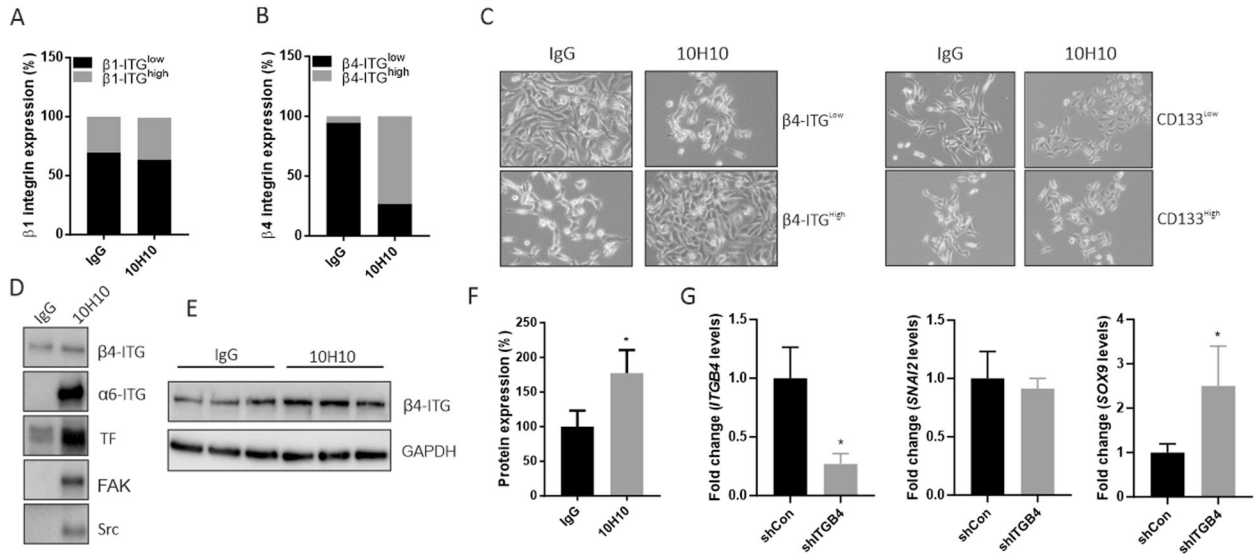

Fig. 5 Inhibition of TF signaling increases expression of, and crosstalk with α6β4-integrin. A, **B** Cells were treated with IgG or Mab-10H10 for 72 h and sorted with MACS antibodies recognizing β1 (**A**) or β4-integrin expression (**B**). **C** One week of cell culture after MACS sorting show morphological changes in β4-integrin^{High} cells. **D** Pull down assay for β4-integrin after Mab-10H10 confirms complex formation with α6-integrin subunit, TF, FAK and Src in MDA-MB-231-mfp cells. **E** Protein expression analysis of β4-integrin in IgG and Mab-10H10 ex vivo cells. **F** Band intensity was quantified using ImageJ software. **G** shRNA-mediated knockdown of β4-integrin knockdown and it effects on expression of *SNAI2* and *SOX9*. MACS and pull down assays were repeated at least three times. Statistical significance was analyzed using Student's *t* test. *$P < 0.05$; **$P < 0.01$; ***$P < 0.001$; ****$P < 0.0001$.

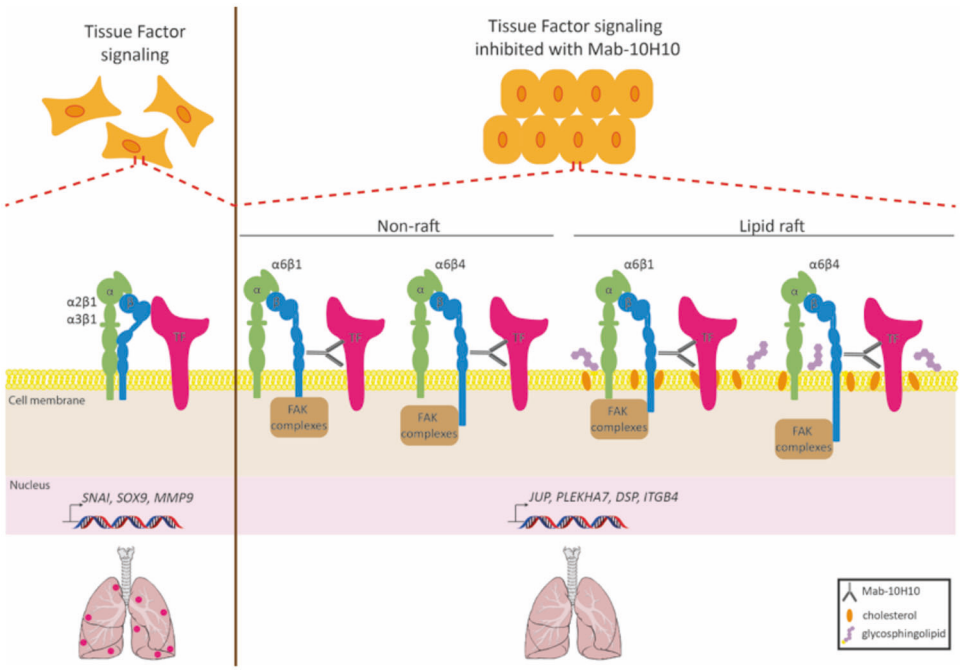

Fig. 6 Schematic overview. Inhibition of TF signaling with Mab-10H10 promotes epithelial cell morphology, with less CSC behavior and metastasis to the lungs. The proposed mechanism comprises disruption of TF/β1-integrin complexes, an increase in β4-integrin expression and formation of focal adhesion complexes by α6β1- and α6β4-integrins.

and Twist expression was determined previously [48]. TF expression in breast specimens was compared to tumor recurrence and/or metastasis. Metastasis-free survival rates were calculated using the Kaplan–Meier method.

In vivo experiments

All animal experiments were approved by the animal welfare committee of the LUMC. Orthotopic injections were performed as described previously [50]. In brief, 5×10^5 MDA-MB-231-mfp cells were mixed with 500 µg Mab-10H10 or isotype matched mouse IgG1 (TIB115) and injected into inguinal fat pads of 6-week-old female NOD-SCID ($n = 4$) or NOD-SCIDγ ($n = 5$) mice (Charles River, Netherlands). Tumor dimensions were measured with a caliper and the volume was calculated ($V = (L \times W^2)/2$), by two independent observers. End points were when control tumors reached ~1000 mm^3 or for humane reasons as defined by institutional guidelines. Tumors and organs were harvested and processed for further analysis. Ex vivo cells were cultured from tumors derived from NOD-SCID mice, by placing 2 mm^3 pieces of tumor on a culture plate in breast cancer cell media (see above). Outgrowing cells were cultured for three weeks and split 3 times per week. After three weeks no murine cells were apparent. Afterwards, ex vivo cells were cultured up to 9 months after isolation.

qPCR

For real time PCR analysis, RNA was isolated using Trisure (Bio-38033, Bioline) and converted to cDNA using the Super Script II kit (18064071, Life Technologies). SYBR select (4472920, Life Technologies) was used to conduct qPCR. See Table S1 for primers. To quantify the presence of human tumor cells in mouse organs, qPCR was performed with the housekeeping genes mouse β-actin and human GAPDH as a measure of metastasis.

Immunoprecipitation and western blotting

Cells were incubated with 50 µg/ml antibodies for 72 h, washed twice in ice-cold HBS and lysed in Brij35-buffer (50 mM Tris, 150 mM NaCl, 1 mM $CaCl_2$, 1 mM $MgCl_2$, 1% Brij35, pH 7.4, cOmplete protease inhibitors (11697498001, Sigma-Aldrich)) for 30 min on ice to collect non-raft fractions. Cells were centrifuged at 800 g for 10 min to pellet cell debris. Supernatant was centrifuged at 16,000 × *g* for 30 min at 4 °C. Pellet was collected and lysed in Brij58-buffer for cholesterol-rich lipid raft fractions, spun at 16,000 × *g* for 30 min. Supernatants of both Brij35- and Brij58 soluble fractions were subjected to immunoprecipitation O/N at 4 °C in the presence of specific antibodies and protein A/G magnetic beads (10001D, 10003D, Invitrogen). After washing steps with lysis buffer, the magnetic beads were resuspended in 2× sample buffer (LC2676, Life Technologies). Western blotting was performed as previously described [51]. Quantification of Western Blot bands for some experiments was performed using Image Lab 5.2 software from Biorad.

Matrigel invasion assay

Cells were serum starved for 24 h, resuspended in serum-free DMEM in the presence of 50 µg/ml antibodies and seeded in the upper compartment of a 24-well invasion chamber (734-1047, BD Biosciences) at 5×10^4 cells/well. The lower compartment was filled with growth medium. Cells invaded for 48 h at 37 °C, fixed in 2% formalin (104002, Merck-Millipore) and stained with 1% crystal violet (C0775-25G, Sigma-Aldrich). Non-invaded cells were removed using a cotton swap; 5 randomly chosen pictures were taken per insert and invaded cells were counted.

Mammosphere and colony formation assay

A single cell suspension was seeded at 500 cells/well in a low-attachment 96 wells plate (CLS3474, Sigma-Aldrich) in mammosphere media (DMEM/F12 phenol-red free (21041-033, Life Technologies), 1% B27 (12587010, Thermo-Fisher Scientific), 20 ng/ml hEGF (E9644, Sigma-Aldrich), 20 ng/ml hFGF (130-093-841, Miltenyi Biotech), 4 µg/ml heparin (LUMC pharmacy), 1% pen/strep). Cells were incubated for 14 days at 37 °C. Spheroids with an area of >2000 μm^2 were counted to determine the mammosphere forming efficiency (MFE).

For colony formation assays, 100 cells were seeded in a 6-wells plate in the presence of 50 µg/ml IgG or 10H10 antibody. Cells were incubated for 14 days at 37 °C, media was refreshed twice weekly. After 2% formalin fixation and crystal violet visualization, holoclones were counted with a colony density of >50 cells.

Immunofluorescent staining

MDA-MB-231-mfp cells were grown on coverslips in the presence of 50 µg/ml antibody for 72 h at 37 °C. Cells were fixed with 2% formalin and permeabilized with 0.1% Triton-X100 (T8787-100ML, Sigma-Aldrich) for 5 min. After 1 h in 5% BSA/PBS blocking-buffer, primary antibody was applied at 50 µg/ml and incubated overnight at 4 °C. Cells were incubated with goat anti-rabbit-Alexa-594 (A-11037, Life Technologies) and phalloidin-FITC (P5282-.1MG, Sigma-Aldrich) for 1 h. Coverslips were mounted with DAPI in ProlongGold (P36931, Thermo-Fisher). Images were captured using a Leica SP5 confocal microscope.

Statistical analysis

Statistical analyses were performed using SPSS software (IBM SPSS Statistics 22, Chicago, USA). Kaplan–Meier analyses and log-rank tests were used to correlate TF expression with metastasis-free survival. Chi-square tests were used to calculate associations between TF expression and expression of stem cell/EMT markers. Data are represented as mean ± SD. Comparisons between data points were done with Student's *t* test for two conditions. With three or more data sets significance was calculated using one-way or two-way ANOVA analysis.

REFERENCES

1. DeSantis C, Ma J, Goding Sauer A, Newman LA, Jemal A. Breast cancer statistics, 2017, racial disparity in mortality by state. CA Cancer J Clin. 2017;67:439–48.
2. Kim DH, Xing T, Yang Z, Dudek R, Lu Q, Chen YH. Epithelial mesenchymal transition in embryonic development, tissue repair and cancer: a comprehensive overview. J Clin Med. 2017;7:1.
3. Lamouille S, Xu J, Derynck R. Molecular mechanisms of epithelial-mesenchymal transition. Nat Rev Mol Cell Biol. 2014;15:178–96.
4. Garg M. Epithelial plasticity and cancer stem cells: Major mechanisms of cancer pathogenesis and therapy resistance. World J Stem Cells. 2017;19:118–26.
5. Ishiwata T. Cancer stem cells and epithelial-mesenchymal transition: novel therapeutic targets for cancer. Pathol Int. 2016;66:601–8.
6. Kotiyal S, Bhattacharya S. Breast cancer stem cells, EMT and therapeutic targets. Biochem Biophys Res Commun. 2014;453:112–6.
7. Gupta PB, Chaffer CL, Weinberg RA. Cancer stem cells: mirage or reality? Nat Med. 2009;15:1010–2.
8. Da Cruz Paula A, Lopes C. Implications of different cancer stem cell phenotypes in breast cancer. Anticancer Res. 2017;37:2173–83.
9. Shibue T, Weinberg RA. EMT, CSCs, and drug resistance: the mechanistic link and clinical implications. Nat Rev Clin Oncol. 2017;14:611–29.
10. Shaker H, Harrison H, Clarke R, Landberg G, Bundred NJ, Versteeg HH, et al. Tissue Factor promotes breast cancer stem cell activity in vitro. Oncotarget. 2017;8:25915–27.
11. Labelle M, Begum S, Hynes RO. Direct signaling between platelets and cancer cells induces an epithelial-mesenchymal-like transition and promotes metastasis. Cancer Cell. 2011;20:576–90.
12. van den Berg YW, Osanto S, Reitsma PH, Versteeg HH. The relationship between tissue factor and cancer progression: insights from bench and bedside. Blood. 2012;199:924–32.
13. Dorfleutner A, Hintermann E, Tarui T, Takada Y, Ruf W. Cross-talk of integrin alpha3beta1 and tissue factor in cell migration. Mol Biol Cell. 2004;15:4416–25.
14. Versteeg HH, Schaffner F, Kerver M, Petersen HH, Ahamed J, Felding-Habermann B, et al. Inhibition of tissue factor signaling suppresses tumor growth. Blood. 2008;111:190–9.
15. Ahamed J, Versteeg HH, Kerver M, Chen VM, Mueller BM, Hogg PJ, et al. Disulfide isomerization switches tissue factor from coagulation to cell signaling. Proc Natl Acad Sci USA. 2006;103:13932–7.
16. Jessani N, Humphrey M, McDonald WH, Niessen S, Masuda K, Gangadharan B, et al. Carcinoma and stromal enzyme activity profiles associated with breast tumor growth in vivo. Proc Natl Acad Sci USA. 2004;101:13756–61.
17. Palumbo JS, Talmage KE, Massari JV, La Jeunesse CM, Flick MJ, Kombrinck KW, et al. Tumor cell-associated tissue factor and circulating hemostatic factors cooperate to increase metastatic potential through natural killer cell-dependent and-independent mechanisms. Blood. 2007;100:133–41.
18. Guo W, Keckesova Z, Donaher JL, Shibue T, Tischler V, Reinhardt F, et al. Slug and Sox9 cooperatively determine the mammary stem cell state. Cell 2012;48:1015–28.
19. Beaver CM, Ahmed A, Masters JR. Clonogenicity: holoclones and meroclones contain stem cells. PLoS ONE. 2014;9:e89834.
20. Schaffner F, Yokota N, Carneiro-Lobo T, Kitano M, Schaffer M, Anderson GM, et al. Endothelial protein C receptor function in murine and human breast cancer development. PLoS ONE. 2013;8:e61071.
21. Kocatürk B, Versteeg HH. Tissue factor-integrin interactions in cancer and thrombosis: every Jack has his Jill. J Thromb Haemost. 2013;11:285–93.
22. Seguin L, Desgrosellier JS, Weis SM, Cheresh DA. Integrins and cancer: regulators of cancer stemness, metastasis, and drug resistance. Trends Cell Biol. 2015;25:234–40.
23. Horton MA. The alpha v beta 3 integrin "vitronectin receptor". Int J Biochem Cell Biol. 1997;29:721–5.
24. Belkin AM, Stepp MA. Integrins as receptors for laminins. Microsc Res Tech. 2000;51:280–301.
25. Marwali MR, Rey-Ladino J, Dreolini L, Shaw D, Takei F. Membrane cholesterol regulates LFA-1 function and lipid raft heterogeneity. Blood. 2003;102:215–22.
26. Rothmeier AS, Liu E, Chakrabarty S, Disse J, Mueller BM, Østergaard H, et al. Identification of the integrin-binding site on coagulation factor VIIa required for proangiogenic PAR2 signaling. Blood. 2018;131:674–85.
27. Bierie B, Pierce SE, Kroeger C, Stover DG, Pattabiraman DR, Thiru P, et al. Integrin-β4 identifies cancer stem cell-enriched populations of partially mesenchymal carcinoma cells. Proc Natl Acad Sci USA. 2017;114:E2337–46.
28. Sawada M, Miyake S, Ohdama S, Matsubara O, Masuda S, Yakumaru K, et al. Expression of tissue factor in non-small-cell lung cancers and its relationship to metastasis. Br J Cancer. 1999;79:472–7.
29. Yamashita H, Kitayama J, Ishikawa M, Nagawa H. Tissue factor expression is a clinical indicator of lymphatic metastasis and poor prognosis in gastric cancer with intestinal phenotype. J Surg Oncol. 2007;95:324–31.

30. Nitori N, Ino Y, Nakanishi Y, Yamada T, Honda K, Yanagihara K, et al. Prognostic significance of tissue factor in pancreatic ductal adenocarcinoma. Clin Cancer Res. 2005;11:2531–9.
31. Seto S, Onodera H, Kaido T, Yoshikawa A, Ishigami S, Arii S, et al. Tissue factor expression in human colorectal carcinoma: correlation with hepatic metastasis and impact on prognosis. Cancer. 2000;88:295–301.
32. Sturm U, Luther T, Albrecht S, Flössel C, Grossmann H, Müller M. Immunohistological detection of tissue factor in normal and abnormal human mammary glands using monoclonal antibodies. Virchows Arch A Pathol Anat Histopathol. 1992;421:79–86.
33. Ueno T, Toi M, Koike M, Nakamura S, Tominaga T. Tissue factor expression in breast cancer tissues: its correlation with prognosis and plasma concentration. Br J Cancer. 2000;83:164–70.
34. Rydén L, Grabau D, Schaffner F, Jönsson PE, Ruf W, Belting M. Evidence for tissue factor phosphorylation and its correlation with protease-activated receptor expression and the prognosis of primary breast cancer. Int J Cancer. 2010;126:2330–40.
35. Zhang X, Li Q, Zhao H, Ma L, Meng T, Qian J, et al. Pathological expression of tissue factor confers promising antitumor response to a novel therapeutic antibody SC1 in triple negative breast cancer and pancreatic adenocarcinoma. Oncotarget. 2017;8:59086–102.
36. Foulkes WD, Smith IE, Reis-Filho JS. Triple-negative breast cancer. N Engl J Med. 2010;363:1938–48.
37. Valastyan S, Weinberg RA. Tumor metastasis: molecular insights and evolving paradigms. Cell 2011;147:275–92.
38. Richards JO, Albers AJ, Smith TS, Tjoe JA. NK cell-mediated antibody-dependent cellular cytotoxicity is enhanced by tamoxifen in HER2/neu non-amplified, but not HER2/neu-amplified, breast cancer cells. Cancer Immunol Immunother. 2016;65:1325–35.
39. Pastushenko I, Brisebarre A, Sifrim A, Fioramonti M, Revenco T, Boumahdi S, et al. Identification of the tumour transition states occurring during EMT. Nature 2018;556:463–8.
40. Magnus N, Garnier D, Meehan B, McGraw S, Lee TH, Caron M, et al. Tissue factor expression provokes escape from tumor dormancy and leads to genomic alterations. Proc Natl Acad Sci USA. 2014;111:3544–9.
41. Yilmaz M, Christofori G. EMT, the cytoskeleton, and cancer cell invasion. Cancer Metastasis Rev. 2009;28:15–33.
42. Chen QK, Lee K, Radisky DC, Nelson CM. Extracellular matrix proteins regulate epithelial-mesenchymal transition in mammary epithelial cells. Differentiation. 2013;86:126–32.
43. Teplyakov A, Obmolova G, Malia TJ, Wu B, Zhao Y, Taudte S, et al. Crystal structure of tissue factor in complex with antibody 10H10 reveals the signaling epitope. Cell Signal. 2017;36:139–44.
44. Ott I, Fischer EG, Miyagi Y, Mueller BM, Ruf W. A role for tissue factor in cell adhesion and migration mediated by interaction with actin-binding protein 280. J Cell Biol. 1998;140:1241–53.
45. Goel HL, Pursell B, Chang C, Shaw LM, Mao J, Simin K, et al. GLI1 regulates a novel neuropilin-2/α6β1 integrin based autocrine pathway that contributes to breast cancer initiation. EMBO Mol Med. 2013;5:488–508.
46. Levy S, Shoham T. Protein-protein interactions in the tetraspanin web. Physiology. 2005;20:218–24.
47. Nisticò P, Di Modugno F, Spada S, Bissell MJ. β1 and β4 integrins: from breast development to clinical practice. Breast Cancer Res. 2014;16:459.
48. van Nes JG, de Kruijf EM, Faratian D, van de Velde CJ, Putter H, Falconer C, et al. COX2 expression in prognosis and in prediction to endocrine therapy in early breast cancer patients. Breast Cancer Res Treat. 2011;125:671–85.
49. Kocatürk B, Van den Berg YW, Tieken C, Mieog JS, de Kruijf EM, Engels CC, et al. Alternatively spliced tissue factor promotes breast cancer growth in a β1 integrin-dependent manner. Proc Natl Acad Sci USA. 2013;110:11517–22.
50. Kocatürk B, Versteeg HH. Orthotopic injection of breast cancer cells into the mammary fat pad of mice to study tumor growth. J Vis Exp. 2015;96:51967.
51. Ünlü B, Bogdanov VY, Versteeg HH. Interplay between alternatively spliced tissue factor and full length tissue factor in modulating coagulant activity of endothelial cells. Thromb Res. 2017;156:1–7.

ACKNOWLEDGEMENTS

We would like to thank Y.W. van den Berg for immunohistochemical staining and E.H. Laghmani for technical assistance.

AUTHOR CONTRIBUTIONS

BÜ, BK, AMdRR, CSL, NS, and RFPvdA performed the experiments, acquired and analyzed data; EJB, IN and DK performed immunohistochemical stainings and analyzed data. PJKK, VYB and WR provided study material and reagents. BÜ and HHV designed the project, wrote the paper and prepared the figures. All authors reviewed and approved the paper.

FUNDING

This study was supported by the Dutch Cancer Society (UL 2015-7594), The Netherlands Organization for Scientific Research (VIDI 91710329) and Worldwide Cancer Research (15-1186). VYB and CSL are partially supported by the NIH/NCI (grant R01CA190717).

COMPETING INTERESTS

The authors declare no competing interests.

ADDITIONAL INFORMATION

Supplementary information The online version contains supplementary material available at https://doi.org/10.1038/s41388-022-02511-7.

Correspondence and requests for materials should be addressed to Henri H. Versteeg.

Reprints and permission information is available at http://www.nature.com/reprints

Publisher's note Springer Nature remains neutral with regard to jurisdictional claims in published maps and institutional affiliations.